

D Hadronic Analyses at CLEO

The CLEO Collaboration

M.S. DUBROVIN

*Department of Physics & Astronomy, Wayne State University,
Detroit, MI 48201*

The CLEO-c results on *D* meson production and hadronic decays obtained with currently available data sets are presented.

1 Introduction

Recent CLEO-c results on *D* meson production and hadronic decays are presented in this overview. The CLEO-c is a general purpose detector at CESR, Cornell Electron-positron Storage Ring. The detector configuration is an upgraded version of the CLEO III¹. In order to run at charm production energy the Silicon Vertex Detector was replaced by the 6 stereo-layers drift chamber; magnetic field in the superconducting solenoid is reduced to 1 T for optimal momentum resolution at lower energy. For stable operation at low energy the 12 superconducting wigglers have been installed at CESR upgrade.

The CLEO-c experimental program² was started in October 2003 and will continue until April 2008. Analyses included in this overview use three samples of events.

- 1) At 3770 MeV we have collected luminosity $\sim 560 \text{ pb}^{-1}$, that corresponds to about 4 M produced $\psi(3770)$ dominantly decaying to $D\bar{D}$ pairs. The 281 pb^{-1} of this sample are processed. We plan to accumulate more data at $\psi(3770)$ by the end of runs.
- 2) The 12 points scan in the range from 3970 to 4260 MeV with total luminosity of $\sim 60 \text{ pb}^{-1}$ is performed in order to find an optimal energy for D_s meson study. We find that the $D_s^\pm D_s^{*\mp}$ cross section is maximal around 4170 MeV.
- 3) At 4170 MeV we have collected 314 pb^{-1} , of which 195 pb^{-1} are processed. At this energy we plan to accumulate 750 pb^{-1} in total.

Below I discuss four topics: *(i)* the absolute D^0 , D^+ , and D_s meson hadronic branching fractions measurement; *(ii)* the $e^+e^- \rightarrow D_{(s)}^{(*)}\bar{D}_{(s)}^{(*)}$ cross section measurement in the energy range from 3970 to 4260 MeV; *(iii)* the inclusive η , η' , and ϕ meson production branching fractions measurement in the D^0 , D^+ , and D_s decays; and *(iv)* the precision D^0 mass measurement. Non-covered recently published results and ongoing analyses are also listed below.

2 Absolute hadronic branching fractions of D^0 and D^+ mesons

The measurement of absolute hadronic branching fractions of D^0 and D^+ meson decays is early published³ for luminosity 56 pb^{-1} . Now it is updated for 281 pb^{-1} . We use technique pioneered by MARK III collaboration: count the yield of the single tags (ST), events where the one side

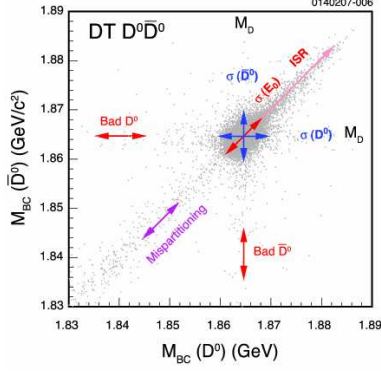


Figure 1: The $m_{BC}(\bar{D})$ vs. $m_{BC}(D)$ distribution in MC.

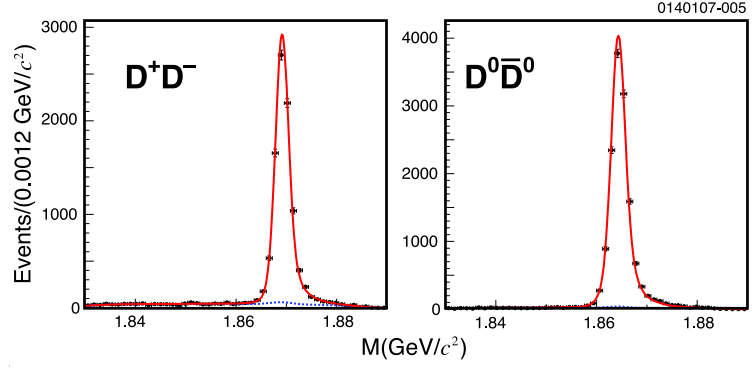


Figure 2: The m_{BC} distributions for DT events combined for all D^0 and D^+ modes.

D of $D\bar{D}$ pair is reconstructed in one of considered hadronic modes, the other side D is ignored; count the yield of the double tags (DT), events where both D mesons are reconstructed in considered hadronic modes. Efficiency is defined from full MC simulation. The total number of $D\bar{D}$ pairs produced and branching fractions are extracted from the χ^2 fit. The yields are defined using the signal variables $\Delta E = E_D - E_{\text{beam}}$ and $m_{BC} = \sqrt{E_{\text{beam}}^2 - P_D^2}$, where E_{beam} is a beam energy, E_D and P_D are the reconstructed D meson candidate energy and momentum, respectively. Typical resolutions are $\sigma(\Delta E) = 7 - 10$ MeV and $\sigma(m_{BC}) = 1.3$ MeV/ c^2 for modes comprising of tracks only. Presence of π^0 meson in the final state degrades resolution by a factor of two roughly. The DT yields are extracted from 2D fit to the $m_{BC}(D)$ versus $m_{BC}(\bar{D})$ distributions. One of them is shown in Fig. 1 for MC events. Fit accounts for m_{BC} resolutions, beam energy spread, ISR, mis-reconstruction of one-side or both D mesons. Projections of the 2D scatter-plots and relevant yields for $D^0\bar{D}^0$ and D^+D^- events are shown in Fig. 2. The ST yields are extracted from fit to the m_{BC} distributions, Fig. 3. We have considered three decay modes for D^0 and six for D^+ meson with largest branching fractions. Fit uses ARGUS function for the background shape and “first principles” in order to parameterize the signal component: the m_{BC} resolution, ISR, Breit-Wigner shape for $\psi(3770)$. The total number of reconstructed ST is $\sim 230K$ for D^0 , and ~ 167 K for D^+ meson. Results for nine branching fractions are shown in Table 1. We compare them with PDG-2004⁴ because PDG-2006⁵ includes our results from 56 pb^{-1} analysis³. The six of measured branching fractions are consistent with the world average values⁴ within one standard deviation, the three – within two standard deviations. Little has changed from 56 pb^{-1} sample, but systematic uncertainties dominate now. It should be noted that the final state radiation (FSR) effect is included in the efficiency calculation. Without

Table 1: Hadronic branching fractions of D^0 and D^+ .

Mode	\mathcal{B} , %
$D^0 \rightarrow K^- \pi^+$	$3.87 \pm 0.04 \pm 0.08$
$D^0 \rightarrow K^- \pi^+ \pi^0$	$14.6 \pm 0.1 \pm 0.4$
$D^0 \rightarrow K^- \pi^+ \pi^+ \pi^-$	$8.3 \pm 0.1 \pm 0.3$
$D^+ \rightarrow K^- \pi^+ \pi^+$	$9.2 \pm 0.1 \pm 0.2$
$D^+ \rightarrow K^- \pi^+ \pi^+ \pi^0$	$6.0 \pm 0.1 \pm 0.2$
$D^+ \rightarrow K_S^0 \pi^+$	$1.55 \pm 0.02 \pm 0.05$
$D^+ \rightarrow K_S^0 \pi^+ \pi^0$	$7.2 \pm 0.1 \pm 0.3$
$D^+ \rightarrow K_S^0 \pi^+ \pi^+ \pi^-$	$3.13 \pm 0.05 \pm 0.14$
$D^+ \rightarrow K^+ K^- \pi^+$	$0.93 \pm 0.02 \pm 0.03$

Table 2: The D_s^+ hadronic branching fractions.

Mode	\mathcal{B} , %
$D_s^+ \rightarrow K_S^0 K^+$	$1.50 \pm 0.09 \pm 0.05$
$D_s^+ \rightarrow K^- K^+ \pi^+$	$5.57 \pm 0.30 \pm 0.19$
$D_s^+ \rightarrow K^- K^+ \pi^+ \pi^0$	$5.62 \pm 0.33 \pm 0.51$
$D_s^+ \rightarrow \pi^+ \pi^+ \pi^-$	$1.12 \pm 0.08 \pm 0.05$
$D_s^+ \rightarrow \pi^+ \eta$	$1.47 \pm 0.12 \pm 0.14$
$D_s^+ \rightarrow \pi^+ \eta'$	$4.02 \pm 0.27 \pm 0.30$

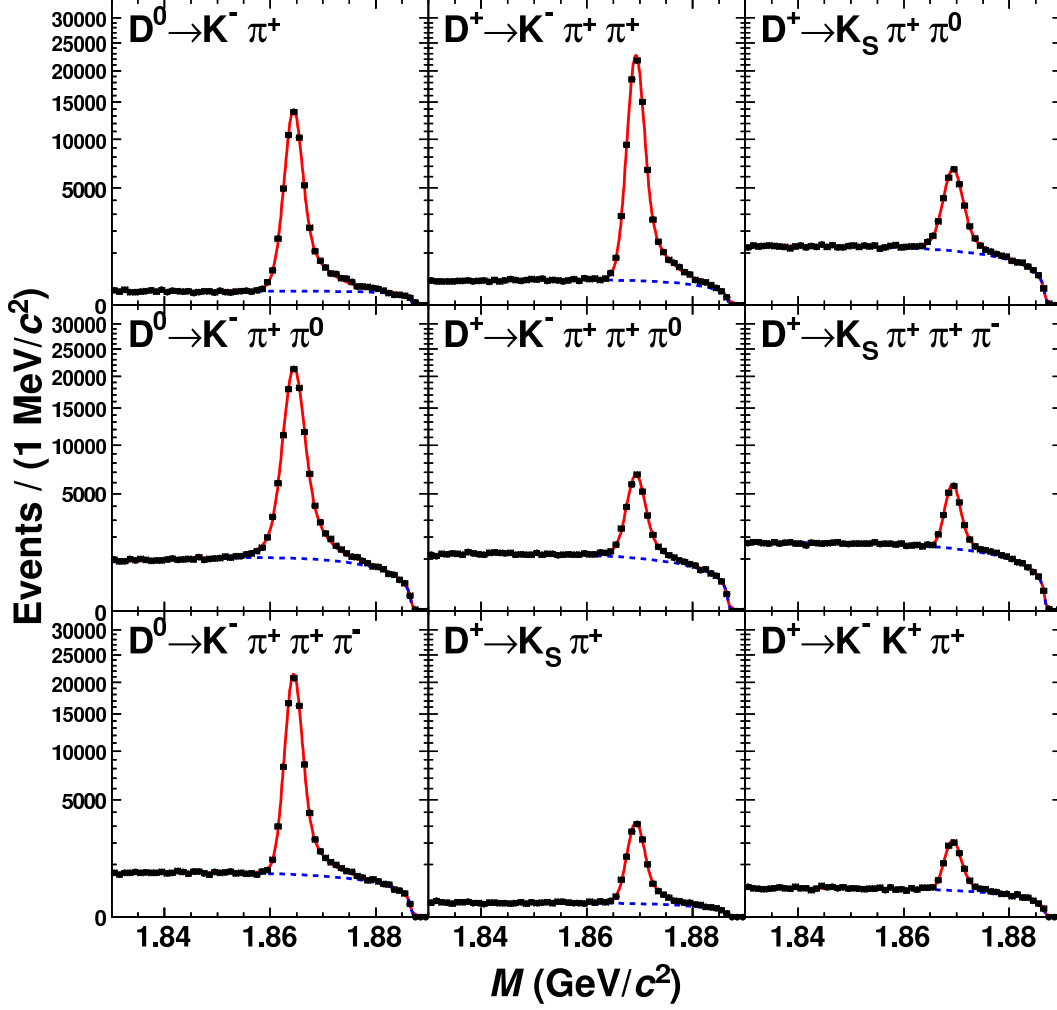


Figure 3: The m_{BC} distributions for three D^0 - and six D^+ -meson decay modes.

account of the FSR the branching fractions decrease up to 2% (depending on mode).

3 D meson pair production cross sections

In order to find an optimal energy for D_s meson study we performed the energy scan with total luminosity of 60 pb^{-1} in 12 points from 3970 to 4260 MeV. We launched this study because in earlier experiments the total hadronic cross section was only measured. We have measured six pair production cross sections, $D\bar{D}$, $D\bar{D}^*$, $D^*\bar{D}^*$, $D_s^\pm D_s^\mp$, $D_s^\pm D_s^{*\mp}$, and $D_s^{*\pm} D_s^{*\mp}$, shown in Fig. 4. The largest D_s meson production rate can be achieved at energy around 4170 MeV in the process $e^+e^- \rightarrow D_s^\pm D_s^{*\mp}$, which cross section reaches 0.9 nb.

4 Absolute D_s hadronic branching fractions

Good kinematic separation between the D meson pair combinations can be achieved if we only reconstruct the D^0 and D^+ candidates and ignore γ and π^0 from D^* and D_s^* decays. It is demonstrated in Fig 5, where the $K^+K^-\pi^+$ invariant mass is plotted *versus* beam constrained mass. Cutting on invariant mass and m_{BC} , Fig. 6 (left), we select events of the process $e^+e^- \rightarrow D_s^\pm D_s^{*\mp}$. In order to measure the D_s meson hadronic branching fractions we use the same

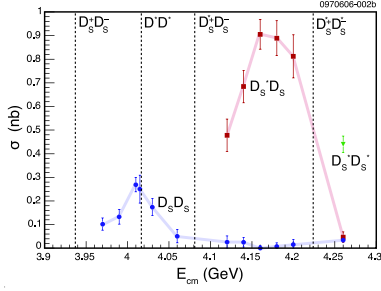


Figure 4: The production cross sections for different D -meson pair combinations.

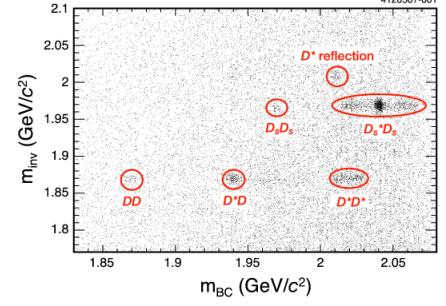
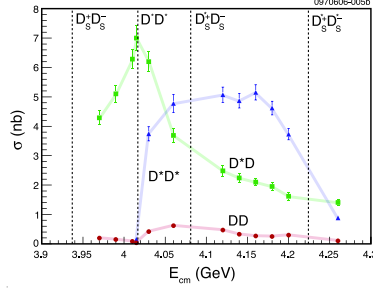


Figure 5: Kinematic separation of the different D -meson pair combinations.

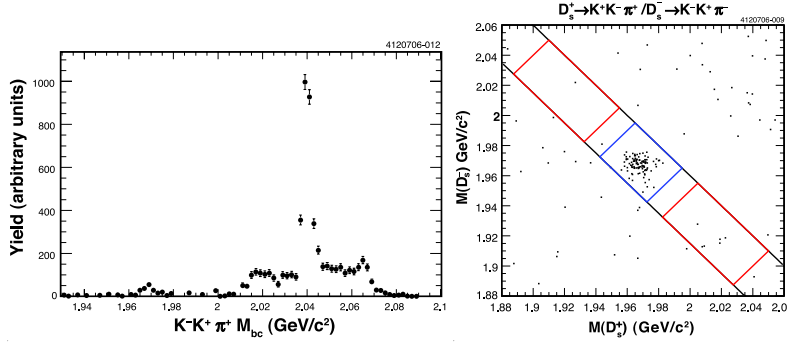


Figure 6: The $m_{BC}(K^- K^+ \pi^+)$ distribution (left), and the 2D invariant mass scatter-plot for DT candidates (right). The central box and two sideband boxes show the signal and background regions, respectively.

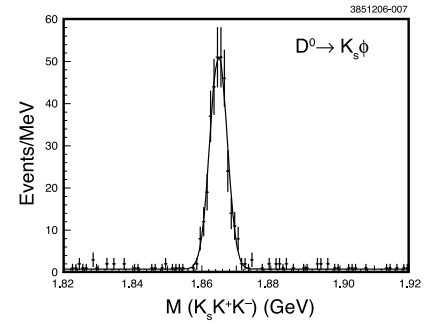


Figure 7: The $K_S^0 K^+ K^-$ invariant mass spectrum.

technique that discussed in Section 2. The number of DT events is counted using the signal and background boxes of the 2D invariant mass distribution, Fig. 6 (right). The number of ST events is extracted from fit to the invariant mass distribution for each of six modes, as shown in Fig. 8 for three of them. Fit uses a linear shape for background and double Gaussian for signal shape. Preliminary results for six D_s modes are shown in Table 2 for 195 pb^{-1} sample. Fair agreement is achieved with results of other experiments⁵ for five available modes.

5 Inclusive branching fractions for η , η' , and ϕ

We have measured the branching fractions for the η , η' , and ϕ mesons inclusive production in D -meson decays. These results are published⁶ for 281 pb^{-1} at $\psi(3770)$ and 195 pb^{-1} at 4170 MeV . We completely reconstruct the tag-side D meson using three decay modes for D^0 , five modes for D^+ , and six modes for D_s^+ meson. Using the rest particles on the other side, we inclusively reconstruct the $\eta \rightarrow \gamma\gamma$, $\eta' \rightarrow \pi^+ \pi^- \eta$, and $\phi \rightarrow K^+ K^-$ decays. Invariant masses are used as a signal variables, as shown for example in Fig. 9. Subtracting background we define relevant yields. Measured branching fractions are shown in Table 3. We noticed that the ϕ meson production branching fractions depend on ϕ momentum. It is also interesting to note how the decay rate depends on presence of the $s\bar{s}$ quarks. The ϕ meson is almost pure $s\bar{s}$ state, η' has a larger $s\bar{s}$ component than η . Table 3 reflects the fact that D_s meson prefers to decay in $s\bar{s}$ -rich states comparing to the D^0 and D^+ mesons.

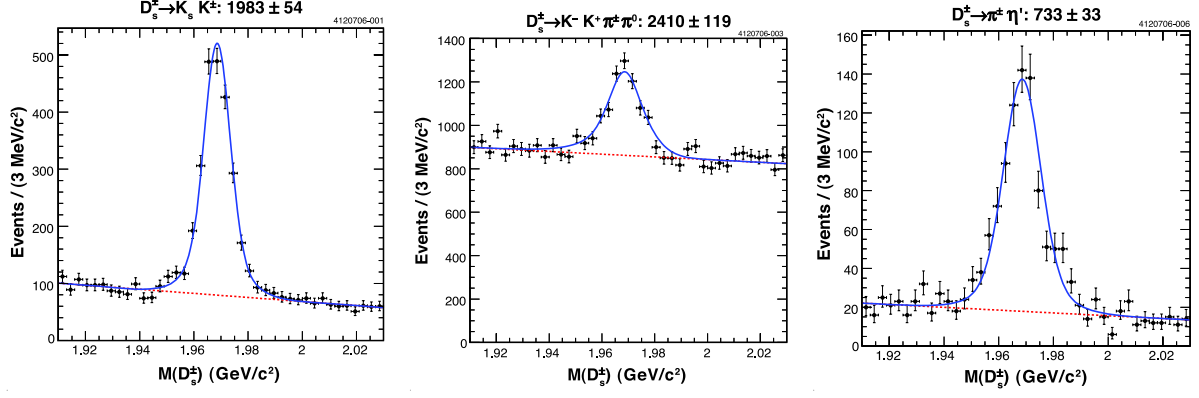


Figure 8: The three of six invariant mass spectra for the ST D_s^+ candidates.

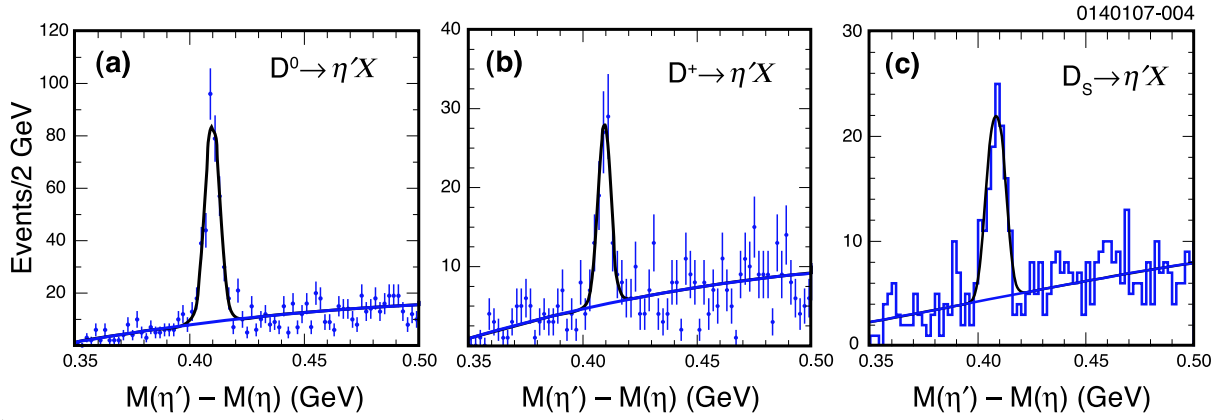


Figure 9: The invariant mass spectra for η' candidates.

6 D^0 meson mass measurement

The precision D^0 mass measurement is recently published⁷. Current mass value⁵ has $0.4 \text{ MeV}/c^2$ uncertainty, that is a result of averaging over several experiments, dominated by the LGW, MARK II, and NA32 measurements. In previous experiments the D^0 mass was measured using the $D^0 \rightarrow K^- \pi^+$ and $D^0 \rightarrow K^- \pi^+ \pi^+ \pi^-$ decays. With 281 pb^{-1} sample we use an advantage of the $D^0 \rightarrow K_S^0 \phi$ decay (mass spectrum is shown in Fig. 7) which has a small energy released, $M(D^0) - M(\phi) - M(K_S) = 347 \text{ MeV}/c^2$, that restricts a momentum range of the final particles, ($400 < P_K, P_\pi < 600$) MeV/c . We estimate a systematic uncertainties in momentum calibration using inclusively reconstructed $K_S^0 \rightarrow \pi^+ \pi^-$ in D meson decays. The maximum uncertainty arises due to the momentum and $\cos \theta$ dependence for π -tracks. The magnetic field calibration is done using invariant mass reconstruction in the decay $J/\psi \rightarrow \mu^+ \mu^-$. We also check the π -meson momentum calibration using invariant mass reconstruction in the decay $\psi(2S) \rightarrow \pi^+ \pi^- J/\psi$. In both cases we rely on high precision mass measurement⁵ of the J/ψ and $\psi(2S)$. We have measured the D^0 meson mass value, $M(D^0) = (1864.847 \pm 0.150_{\text{stat.}} \pm 0.095_{\text{syst.}}) \text{ MeV}/c^2$, with statistical and systematic uncertainty a few times smaller than the world average.

7 Non-covered results on D -meson hadronic decays

Several topics, listed below, have not been covered in this overview. Two papers have been recently published, “Branching fraction for the DCSD $D^+ \rightarrow K^+ \pi^-$ ”⁸, and “Measurement of interfering $K^{*+} K^-$ and $K^{*-} K^+$ amplitudes in the decay $D^0 \rightarrow K^+ K^- \pi^0$ ”⁹. The results of

Table 3: Inclusive branching fractions (in %) of D meson decays and their ratios.

Mode	ηX	$\eta' X$	ϕX
D^0	$9.5 \pm 0.4 \pm 0.8$	$2.48 \pm 0.17 \pm 0.21$	$1.05 \pm 0.08 \pm 0.07$
D^+	$6.3 \pm 0.5 \pm 0.5$	$1.04 \pm 0.16 \pm 0.09$	$1.03 \pm 0.10 \pm 0.07$
D_s^+	$23.5 \pm 3.1 \pm 2.0$	$8.7 \pm 1.9 \pm 0.8$	$16.1 \pm 1.2 \pm 1.1$
D_s^+/D^0	$2.47 \pm 0.34 \pm 0.18$	$3.51 \pm 0.80 \pm 0.27$	$15.3 \pm 1.6 \pm 0.8$
D_s^+/D^+	$3.73 \pm 0.57 \pm 0.27$	$8.37 \pm 2.23 \pm 0.64$	$15.6 \pm 1.9 \pm 0.8$

several analyses are expected to be presented shortly: the D^0 , D^+ , and D_s hadronic branching fraction measurements for single and double Cabibbo suppressed decays; the quantum correlation analysis of the $D^0\bar{D}^0$ decays; the Dalitz plot analyses of the decays $D^+ \rightarrow K^-\pi^+\pi^+$, $D^+ \rightarrow \pi^-\pi^+\pi^+$, $D_s^+ \rightarrow K^-K^+\pi^+$, $D^0 \rightarrow K_{(S,L)}^0\pi^+\pi^-$, $D^0 \rightarrow K_S^0\pi^0\pi^0$, etc., with and without CP and flavor tags.

8 Summary

In summary, CLEO-c experiment is taking data from October 2003 until April 2008. We have collected 4 M of $D\bar{D}$ pairs, 0.3 M of $D_s^\pm D_s^{*\mp}$ pairs at $\sqrt{s} = 4170$ MeV, and 28 M of $\psi(2S)$. We expect to collect more data in the same energy regions by the end of runs at CESR. Preliminary results on D meson production and decays are presented. In most measurements we have reached better precision than the world average.

References

1. G. Viehhauser, *CLEO III Operation, Nucl. Instrum. Methods A* **462**, 146 (2001).
2. CLEO-c and CESR-c: A New Frontier of Weak and Strong Interactions, CLNS-01/1742.
3. Q. He, et al. (CLEO Collaboration), *Phys. Rev. Lett.* **95**, 121801 (2005).
4. S. Eidelman et al, *Phys. Lett. B* **592**, 1 (2004).
5. W.-M. Yao et al., *Journal of Physics G* **33**, 1 (2006).
6. G. S. Huang et al. (CLEO Collaboration), *Phys. Rev. D* **74**, 112005 (2006).
7. C. Cawlfeld et al. (CLEO Collaboration), *Phys. Rev. Lett.* **98**, 092002 (2007).
8. S. A. Dytman et al. (CLEO Collaboration), *Phys. Rev. D* **74**, 071102 (2006).
9. C. Cawlfeld et al. (CLEO Collaboration), *Phys. Rev. D* **74**, 031108 (2006).